

Outflowing protons and heavy ions as a source for the sub-keV ring current

T. T. Giang¹, M. Hamrin², M. Yamauchi¹, R. Lundin¹, H. Nilsson¹, Y. Ebihara³, H. Rème⁴, I. Dandouras⁴, C. Vallat⁵, M. B. Bavassano-Cattaneo⁶, B. Klecker⁷, A. Korth⁸, L. M. Kistler⁹, and M. McCarthy¹⁰

¹Swedish Institute of Space Physics, Kiruna, Sweden

²Department of Physics, Umeå University, Umeå, Sweden

³Institute for Advanced Research, Nagoya University, Japan

⁴Centre d'Etude Spatiale des Rayonnements, Toulouse, France

⁵VEGA contracted to Solar System Science Operations Division, ESA/ESAC, Madrid, Spain

⁶L'Istituto di Fisica dello Spazio Interplanetario, Roma, Italy

⁷Max Planck Institute for Extraterrestrial Physics, Garching, Germany

⁸Max-Planck-Institut für Sonnensystemforschung, Katlenburg-Lindau, Germany

⁹University of New Hampshire, Durham, New Hampshire, USA

¹⁰University of Washington, Seattle, USA

Received: 8 April 2008 – Revised: 14 January 2009 – Accepted: 22 January 2009 – Published: 19 February 2009

Abstract. Data from the Cluster CIS instrument have been used for studying proton and heavy ion (O^+ and He^+) characteristics of the sub-keV ring current. Thirteen events with dispersed heavy ions (O^+ and He^+) were identified out of two years (2001 and 2002) of Cluster data. All events took place during rather geomagnetically quiet periods. Three of those events have been investigated in detail: 21 August 2001, 26 November 2001 and 20 February 2002. These events were chosen from varying magnetic local times (MLT), and they showed different characteristics.

In this article, we discuss the potential source for sub-keV ring current ions. We show that: (1) outflows of terrestrial sub-keV ions are supplied to the ring current also during quiet geomagnetic conditions; (2) the composition of the outflow implies an origin that covers an altitude interval from the low-altitude ionosphere to the plasmasphere, and (3) terrestrial ions are moving upward along magnetic field lines, at times forming narrow collimated beams, but frequently also as broad beams. Over time, the ion beams are expected to gradually become isotropised as a result of wave-particle interaction, eventually taking the form of isotropic drifting sub-keV ion signatures. We argue that the sub-keV energy-time dispersed signatures originate from field-aligned terrestrial ion energising and outflow, which may occur at all local times and persist also during quiet times.

Keywords. Magnetospheric physics (Magnetosphere-ionosphere interactions; Magnetospheric configuration and dynamics; Plasma convection)

1 Introduction

The ring current consists of particles trapped in the geomagnetic field. The ring current varies with time and causes a slight decrease of the Earth's surface magnetic field during magnetic storms (Williams, 1983). Energetic ions drift westwards due to the gradient-curvature drift being larger than the $\mathbf{E} \times \mathbf{B}$ drift ($v = \frac{m}{2qB^2}(v_{\perp}^2 + 2v_{\parallel}^2)e \times \nabla_{\perp} \mathbf{B} - \mathbf{E} \times \mathbf{B}$), while the eastward $\mathbf{E} \times \mathbf{B}$ drift dominates electrons and low energy ions. For intermediate energies, the drift motion is more complex, and the ions experience a competition between the gradient-curvature and $\mathbf{E} \times \mathbf{B}$ drift, with the gradient-curvature drift slowing down the eastward $\mathbf{E} \times \mathbf{B}$ motion. Eastward-drifting low-energy ions are predominantly of ionospheric origin; therefore, the issue of the low-energy wedge-like structures (energy-latitude dispersion structures) discussed by Yamauchi et al. (1996, 2005, 2006) and Ebihara et al. (2001) is largely a matter of the sources and losses of the ionospheric plasma.

The knowledge of heavy ionospheric ions in the ring current and plasma sheet dates back to the early 1970s. The first observations of energetic ionospheric heavy ions in the magnetosphere were made by Shelley et al. (1972). The data was



Correspondence to: T. T. Giang
(tony.giang@irf.se)

obtained from a set of ion mass spectrometers that covered the energy range from 0.7 keV to 12 keV on board the polar-orbiting satellite 1971-089A. This satellite had a nearly circular orbit with an altitude at 800 km covering 03:00–15:00 local time (LT). They concluded that the observed precipitation of heavy ions (O^+) is of ionospheric origin. Since then, a number of observations pertaining to the contribution of heavy ionospheric ions to the ring current have been made.

This study is concerned with the details of sub-auroral sub-keV ions. Studies of this region have been made by, e.g., GEOS-1 and Prognoz-7. Geiss et al. (1978) and Balsiger et al. (1980) used data from the Ion Composition Experiment (ICE) onboard the GEOS-1 spacecraft. Regarding the thermal plasmasphere population (~ 1 eV/e), they found that it comprised of H^+ , O^+ , He^+ , D^+ , He^{2+} and O^{2+} ions, with a predominance of H^+ , He^+ and O^+ in order of abundance. For the low-energy ions, they found that H^+ dominates over the heavy ions during magnetically quiet periods. Both Geiss et al. (1978) and Balsiger et al. (1980) concluded that the solar wind and the ionosphere are the two major sources of hot plasma in the magnetosphere. Regarding more energetic ions, Balsiger et al. (1980) and Lundin et al. (1980) found a strong depletion of H^+ ions in the inner ring current as a result of charge-exchange (Tinsley, 1981), leaving the inner part of the ring current dominated by heavy ionospheric ions. However, while these heavy ions are the remains of past ionospheric ion outflow, little is known regarding sub-auroral latitudes as a region of ionospheric ion outflow. Chappell et al. (1982) made observations of the pitch-angle distribution and ion composition of thermal plasma in the inner magnetosphere using the Retarding Ion Mass Spectrometer (RIMS) instrument on board the Dynamics Explorer satellite (DE-1). The energy range of the data is up to 50 eV. They found complex characteristics of the ions, including field-aligned distributions, suggesting that the magnetosphere is fed by ions from the ionosphere and plasmasphere. Horwitz (1987) proposed an additional injection path from the dayside cleft-region into the inner magnetosphere, introducing the notion of “core plasma” for low-energy ions populating the inner magnetosphere.

Regarding ion precipitation, Sauvaud et al. (1981) observed two types of ion precipitation in the auroral and sub-auroral night-time zone (approximately 00:00–06:00 MLT) using the data from the polar orbiting satellite Aureol 1 (apogee at 2500 km and perigee at 411 km). The energy range for the measured auroral ions is from 0.4 keV to 30 keV. They concluded that the low-energy ions observed at sub-auroral latitudes are related to the eastward drift of trapped particles originating from the injection boundary during increasing AE index, i.e., when plasma sheet ions are injected into the inner magnetosphere. Using data from the F6 and F7 DMSP spacecraft, which have a sun-synchronous (08:30 MLT) circular polar orbit at 850 km altitude, Newell and Meng (1986) observed isolated and latitudinal narrow regions of ion precipitation with energies up to 1 keV in

the sub-auroral region. They concluded that cold plasma from the plasmasphere can be mixed with the warm magnetospheric plasma during substorm activities and transported from post midnight to circa 08:30 MLT.

The sub-keV ions in the inner magnetosphere region have been investigated using data from the P78-2 satellite. This satellite was in an elliptical equatorial orbit with an apogee of $\sim 7.8 R_E$ and a perigee of $\sim 5.3 R_E$. The studies showed that the low-energy ion distributions are field-aligned, while the high-energy ions are peaked perpendicular to the magnetic field (Fennell et al., 1981; Kaye et al., 1981). The distributions were named ion “zipper” distributions due to a peculiar zipper-like feature observed in the ion spectrograms at the transition (in energy) from predominantly field-aligned fluxes to predominately trapped fluxes. The field-aligned ion distributions will become isotropised over time and give rise to ion energy-latitude dispersed structures, denoted as wedge-like structures by Yamauchi et al. (1996, 2005, 2006). Observations by Fenell et al. (1981) and Kaye et al. (1981) were carried out at L-values ~ 5.5 – 7.7 and during all magnetic local times. The authors concluded that the source of the high-energy ions is the plasma sheet, while the low-energy ions are of ionospheric origin.

Yamauchi et al. (1996) observed energy-latitude dispersive structures of trapped ions in the sub-keV energy range inside the ring current region. These wedge-like structures are frequently observed in the dayside sub-auroral region. Recently, statistical studies were performed on the occurrence of the wedge-like structures at different altitudes and different local times. Satellites such as Viking (mid-altitude at 5000–13 000 km), Freja (1600 km) and the Cluster satellites ($>4 R_E$) (Yamauchi et al., 1996, 2005, 2006; Ebihara et al., 2001, 2008; Yamauchi and Lundin, 2006) have been used for this purpose. All observations showed that the occurrence probability of wedge-like structures gradually decreases from morning to noon and from noon to evening, with the peak in the early morning sector.

Using a particle drift simulation, Ebihara et al. (2001) reproduced the wedge-like structures of the sub-keV ions during geomagnetic disturbed conditions by assuming that (1) the source ions are injected from the near-Earth tail to the midnight sector, (2) the source distribution function in the midnight ($L=10$) is isotropic Maxwellian with a temperature of 5 keV and number density of 0.3 cm^{-3} , and (3) the ions are drifting in a co-rotational electric field, a dipole magnetic field and the Volland-Stern type convection electric field (Volland, 1973; Stern, 1975; Maynard and Chen, 1975). In their particle drift simulation, they observed three types of wedge-like structures, which were named types 1, 2 and 3, each exhibiting different characteristics. Type 1: the energy increases with invariant latitude (ILAT); Type 2: the energy increases with ILAT and then subsequently decreases with ILAT; Type 3: the energy decreases with ILAT. The successful reproduction of the dispersion patterns by Ebihara et al. (2001) indicates that the wedge-like structures could be

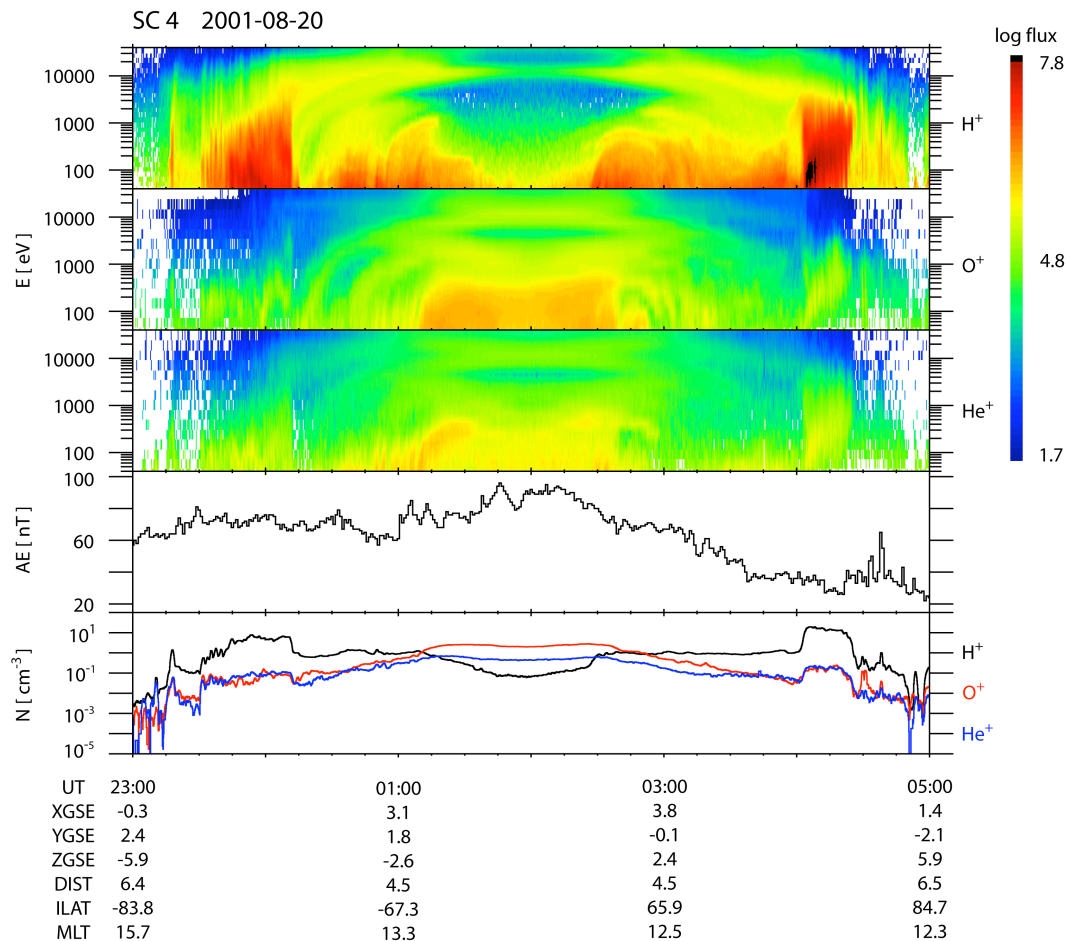


Fig. 1. Energy-time spectrograms over 4π average differential fluxes in $[(\text{cm}^2 \text{ sr keV})^{-1}]$, AE and density plot of H^+ , O^+ and He^+ in the energy range of 0.04 keV to 40 keV for the entire pericentre pass of the 20–21 August 2001.

related to past substorm activities many hours before. Vallat et al. (2007) have also reproduced some of the dispersive ion structures by using numerical simulations of particle trajectories.

Yamauchi and Lundin (2006) confirmed that the wedge-like structures are related to past AE activities, and that the wedge-like trapped ions at mid-latitudes are most likely the same as the detached ions in the sub-auroral region observed by polar orbiting satellites as described above. They found that there is no relation between the wedge-like structures and D_{st} indices. They also raised questions on (1) the source location and (2) the drift velocity. The drift time from the source to the dayside statistically obtained from their backward superposed epoch analyses is much shorter (by a factor of 2–3) than in the simulation by Ebihara et al. (2001) with nearly zero lag time from substorm onset to the appearance of the wedge-like structure in the morning sector (Yamauchi and Lundin, 2006).

Yamauchi and Lundin (2006) also found that the wedge-like structures seen in the evening sector have travelled from

the morning sector by an eastward drift beyond what the model predicts. Their statistics indicate that a substantial percentage of these structures are instead formed in the morning sector during substorms. They could not identify the absolute source locations and the formation processes of the source particles (O^+ and H^+). The source problem is again discussed by Yamauchi et al. (2006) using Cluster data, confirming that some of the structures must have begun to form their energy dispersion in the morning sector. They also suggested that the O^+ and H^+ sources might not be located at the same magnetic local time. The source problem might also be related to the O^+/H^+ ratio problem reported in Yamauchi et al. (2005).

To elucidate the source problem, i.e., from where the O^+ and H^+ ions originate, we studied in more detail CIS-data from three Cluster orbits (two dayside and one nightside, see Fig. 2) during relatively quiet times when the convection electric field is expected to be weaker and more stable. We investigated possible plasma source regions for the sub-keV ring current ions by analysing in more detail the pitch-angle

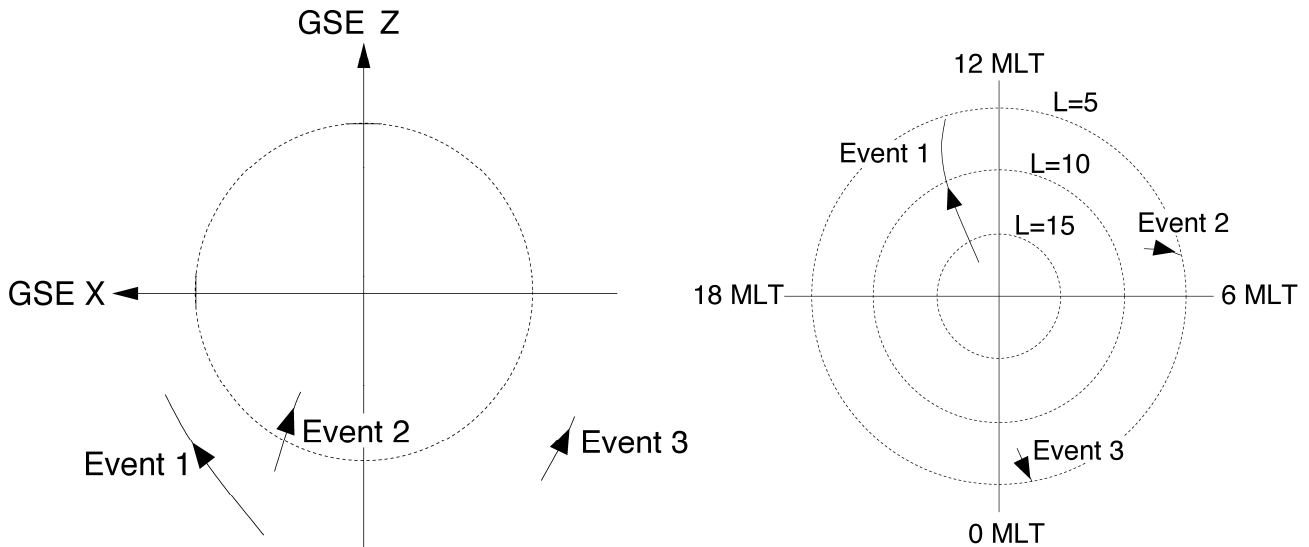


Fig. 2. Orbit projection sketches of the three traversals in X-Y GSE and MLT-L shell. For more details, see Table 1.

distributions of H^+ , O^+ and He^+ and comparing their density and upgoing flux ratios. In a statistical study of ring current H^+ and O^+ by Collin et al. (1993), some of the issues addressed here were also discussed. However, their instrument measured higher energies >110 eV, and they did, for instance, not discuss time dispersion and ion outflow signatures. In this paper, we show that the upgoing ion fluxes are usually associated with energy-time dispersions signatures.

The Cluster spacecraft are placed in a polar orbit with an apogee of $\sim 18.7 R_E$ and a perigee of $\sim 4 R_E$. This means that the Cluster spacecraft can reach deeper into the magnetosphere compared to the P78-2 satellite used in some earlier studies of the 1980s. In this article, the bidirectional ion outflow (upgoing ions from the Northern and Southern Hemispheres) and its relation to the evolution of sub-keV ions in the ring current are of particular interest. All three events were observed during magnetically quiet periods.

2 Instrumentation

We use data from the Cluster Ion Spectrometry (CIS) instrument on board the Cluster II spacecraft (SC 1, SC 3 and SC 4). CIS is an ion plasma spectrometry package capable of obtaining full three-dimensional ion distributions with good time resolution and with mass-per-charge composition determination. The CIS package consists of two different instruments, a time-of-flight ion Composition Distribution Function (CODIF), which can resolve the major magnetospheric ions, and a Hot Ion Analyser (HIA), which has no mass resolution but higher energy and angular resolution, as well as a Data Processing System (DPS), which permits on-board data processing. By using a time-of-flight technique,

CODIF can resolve H^+ , He^+ , He^{2+} and O^+ . CODIF covers a 2π field-of-view orthogonal to the spin plane with 16 detectors. This gives us the angular resolution of 22.5° in the spin plane. More detailed descriptions of the CIS instruments can be found in Rème et al. (2001).

3 Observations

We have examined two years (2001 and 2002) of Cluster CIS CODIF data of hydrogen (H^+), oxygen (O^+) and helium (He^+) ions in the sub-keV energy range, 40–200 eV. In our data base, we have over 200 perigee traversals. From these traversals, we chose three events to investigate in more detail: 21 August 2001, 26 November 2001, and 20 February 2002. All three events were observed during different magnetic local times and with different L values (14.0–13.2 MLT and $45\text{--}10 R_E$; 7.1–6.9 MLT and $11\text{--}6.5 R_E$; 0.6–0.7 MLT and $8\text{--}5 R_E$), but they all showed plasma outflow along magnetic field lines during low geomagnetic activities. This suggests an almost continuous supply of energised ionospheric ions into the ring current for all MLT and during magnetically quiet periods. Figure 2 shows the orbit projection in GSE X-Y and in MLT-L shell of our three events. From our observation, we will also be able to draw conclusions regarding the source of these upgoing ions.

The top three panels of Fig. 1 show the H^+ , O^+ and He^+ energy-time spectrograms for the entire pericentre pass of the 21 August event. The two bottom panels in Fig. 1 show the AE index and the number density of H^+ , O^+ and He^+ ions in the energy range 40–40 000 eV. From the spectrograms, one may also distinguish energy-time dispersed structures as reported by Yamauchi et al. (1996). It should be noted,

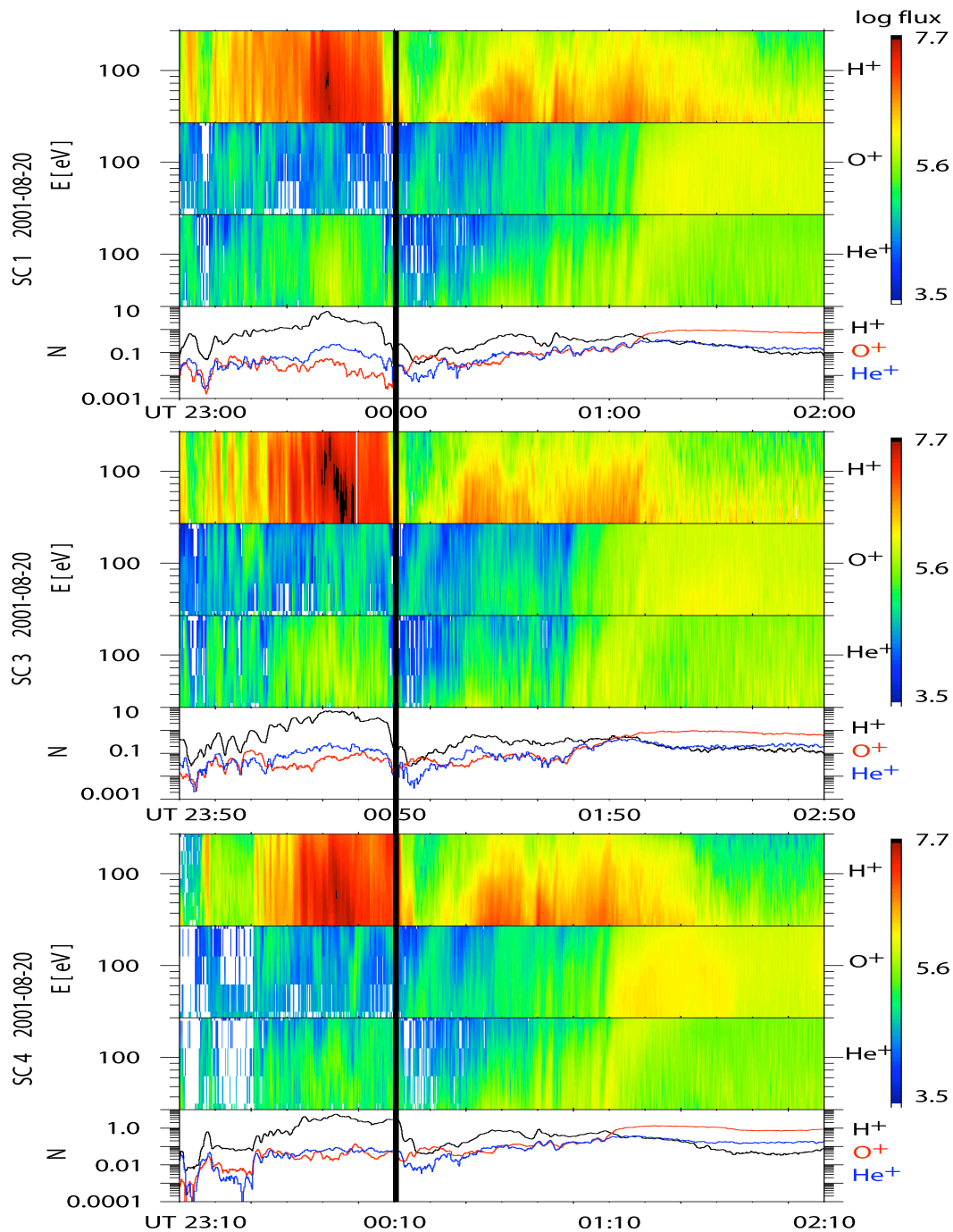


Fig. 3. H^+ , O^+ and He^+ energy-time spectrograms in $[(\text{cm}^2 \text{ s sr keV})^{-1}]$ for 20–21 August 2001 in the energy range of 0.04 keV to 0.2 keV. The spectrograms and number density in $[\text{cm}^{-3}]$ plots are time-shifted for the Cluster spacecraft, SC 3 and SC 4 compare to SC 1. The black line indicates the same energy-time dispersed signature for O^+ .

however, that our focus is not on the energy-time dispersed signatures as such, but rather on the ion outflow signatures related with them. A strong decrease/void of energetic H^+ can be seen near the pericentre, as shown in Fig. 1. This is most likely an effect of charge exchange, removing keV H^+ more

effectively than O^+ and He^+ (e.g. Tinsley, 1981; Roelof et al., 1985). The H^+ charge exchange cross-section is much higher than the O^+ and He^+ cross-sections. The data in Fig. 1 are from a geomagnetically quiet period, the last sub-storm injection being some 72 h ago; i.e. there is sufficient

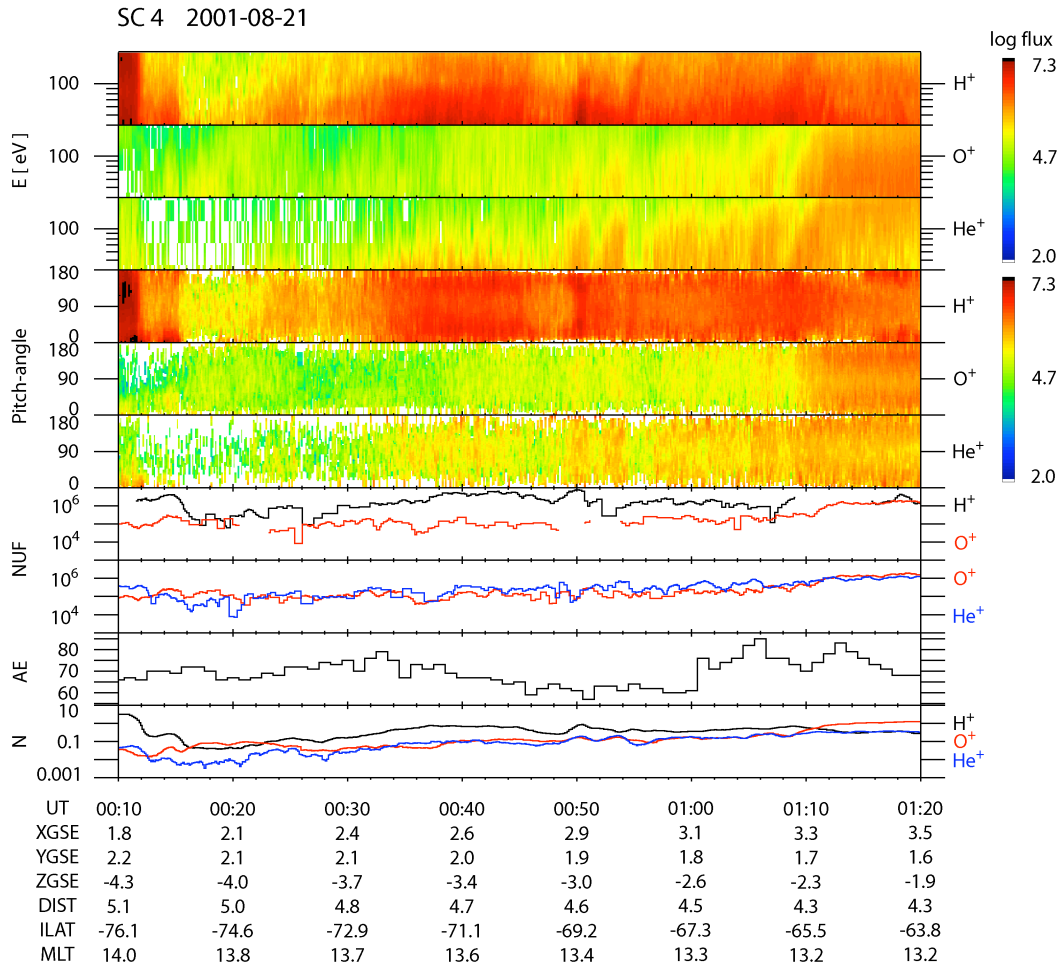


Fig. 4. Energy-time spectrograms, pitch-angle distributions [$(\text{cm}^2 \text{sr keV})^{-1}$], net upcoming fluxes (NUF) in [$\text{cm}^{-2} \text{s}^{-1}$], AE in [nT] and density plot in [cm^{-3}] in the energy range of 40 eV to 200 eV (low energy) for H^+ , O^+ and He^+ during the period from 00:10 UT through 01:20 UT, on 21 August 2001.

time for charge-exchange to remove a large fraction of the keV H^+ . From the bottom panel of Fig. 1, we also note that the He^+ content is relatively high compared to O^+ , except in the inner ring current, where O^+ is the most abundant ion species. This is another indication of charge exchange.

As already noted, all three events to be discussed in this article took place during relatively quiet periods, as seen from the AE indices displayed in the figures and IMF discussed. The median and mean values of the 13 D_{st} indices were -8 nT and -15 nT , respectively, which is another indication of relatively quiet conditions. Moreover, the values of 2 out of 13 of the D_{st} indices were even positive (8 June 2001 and 21 August 2001).

3.1 Event 1: 21 August 2001

Figure 3 shows a zoom in the H^+ , O^+ and He^+ energy-time spectrograms and density of 21 August 2001. The MLT is approximately 14.0–13.2. The spectrograms and densities were

calculated in the low energy range of 0.04 keV–0.2 keV. The spectrograms and density plots are time shifted for the Cluster spacecraft 3 and 4 to be comparable with spacecraft 1. One can recognise some minor differences between the three spacecraft. Even if there are some spatial and temporal differences between the spacecraft (even after time shifting), the overall appearances of the energy-time dispersed signatures are the same for all three spacecraft. Hence, we conclude that these energy-time dispersed signatures are rather stationary in time. Since the data are very similar on all spacecraft, we chose only to investigate data from SC 4.

Figure 4 shows the energy-time spectrograms, pitch-angle distributions of the differential flux, net upcoming flux and density plots for H^+ , O^+ and He^+ ions during the period from 00:10 UT through 01:20 UT, on 21 August 2001. In the low energy data (0.04 keV–0.2 keV) presented in the top three panels of Fig. 4, one can recognise clear energy-time dispersed signatures for H^+ , O^+ and He^+ ions in two time

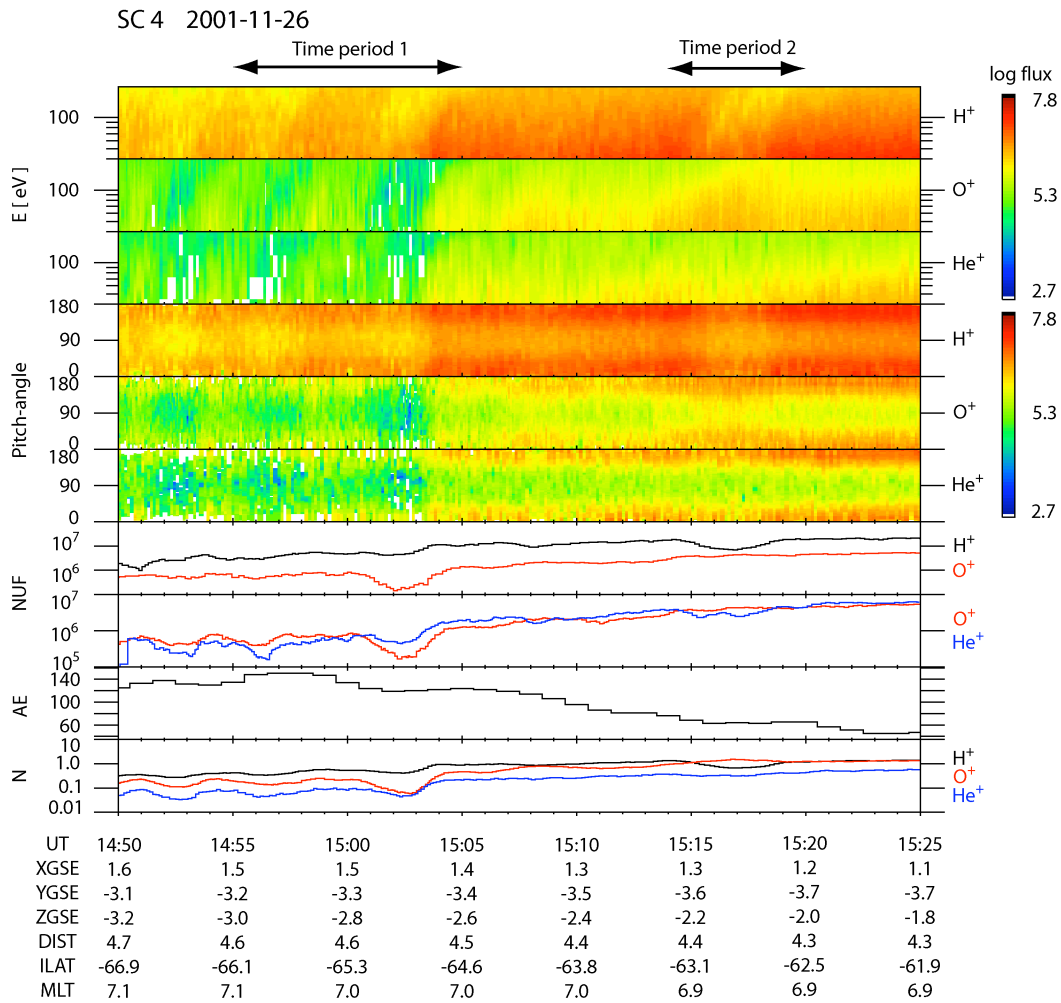


Fig. 5. Energy-time spectrograms, pitch-angle distributions $[(\text{cm}^2 \text{ s sr keV})^{-1}]$, net upgoing fluxes (NUF) in $[\text{cm}^{-2} \text{ s}^{-1}]$, AE in [nT] and density plot in $[\text{cm}^{-3}]$ in the low energy range of 40 eV to 200 eV for H^+ , O^+ and He^+ during the period from 14:50 UT through 15:25 UT, on 26 November 2001.

intervals, 00:39 UT–00:50 UT and 00:52 UT–01:09 UT. The following assumptions are made in computing the net upgoing flux of planetary ions.

1. Energising of planetary ions may take place at all altitudes, from the lower ionosphere to the high-altitude ionosphere/plasmasphere.
2. Ion energising is primarily driven by waves (see, e.g. Moore et al., 1999, for a review). Transverse (to the magnetic field) energising of ions by waves leads to a diverging magnetic dipole field and, eventually, to a “conical” distribution.
3. Further energising and wave-broadening with altitude leads to further widening of the “ion conics,” such that instead of a beam-like folded conic, a wider beam with respect to pitch angle forms (see, e.g., panels 5 and 6

in Fig. 5). An ion source close to the magnetic equator (e.g., plasmasphere) leads to even broader outflow beams.

4. Because the observations are made on closed field lines (Ring Current), ion outflow, as a consequence of wave energising, is expected to reach the equatorial plane from both hemispheres.
5. The net planetary ion outflow is determined by adding the hemispherical outflow. We then subtract the flux of trapped particles (60° – 120° pitch-angle) from the outflowing particle flux (0° – 60° ; 120° – 180°). Integrating over these angles, one finds that an isotropic distribution leads to zero upgoing flux, while, as in these cases, a bidirectional outflow superposed on an isotropic distribution gives a net upgoing flux.

Table 1. summarises the observations of characteristics from the three events.

Date	MLT	L	D_{st} index	Solar wind
21 Aug 2001	14.0–13.2	17.4–5.1	9 nT→17 nT	IMF $B_Z \sim 0.6$ nT
26 Nov 2001	7.1–6.9	6.5–4.5	–54 nT→–50 nT	IMF $B_Z \sim 0.3$ nT
20 Feb 2002	0.6–0.7	5.9–4.6	–9 nT→–7 nT	IMF $B_Z \sim \pm 1$ nT

The number density plot in the bottom panel of Fig. 4 shows a large amount of He^+ between 00:34 UT and 01:12 UT. Panel 8 displays a corresponding increase of the He^+ during this time period. A large amount of He^+ suggests a plasmaspheric or a high altitude ionospheric origin, where He^+ may be more abundant than O^+ . Panels 4–6 in Fig. 4, showing the H^+ , O^+ and He^+ pitch-angle distributions and the corresponding net upgoing fluxes (panel 8), are revealing in this context. We note here that the pitch-angle distributions in the high-energy range (not shown here) are either isotropic or peaked near 90° . Conversely, the H^+ and He^+ low-energy ion distributions are strongly bidirectional, mixed with an isotropic H^+ component. Panels 7–8 show, therefore, that there is a net upgoing flux of low-energy planetary ions into the ring current. The co-existence of field-aligned and isotropic distributions implies two plasma populations, upgoing plasma (magnetically connected to the source) and pre-existing isotropic drifting plasma, in other words, upgoing planetary plasma mixing with pre-existing sub-keV ring current plasma. Notice also that the dispersion signature (Fig. 4) may in this case be interpreted as the low-energy part of drifting energy-time dispersed signatures as well as a signature of direct outflow of ionospheric plasma into the ring current.

This event is observed during magnetically quiet conditions. Investigating the magnetic indices, we found that $D_{st} \approx 17$ nT (Table 1) during the event. The AE values displayed in panel 9 in Fig. 4 were rather small. IMF measured by the Advanced Composition Explorer (ACE) was weakly positive, ($B_z \sim 0.6$ nT, Table 1).

3.2 Event 2: 26 November 2001

Figure 5 shows similar data as in Fig. 4, but in this case for 26 November 2001, during 14:50–15:25 UT. MLT during the time interval varied between 7.1 and 6.9. Clear energy-time dispersed signatures occurred during two periods: 14:55 UT–15:05 UT (time period 1) and 15:14 UT–15:20 UT (time period 2).

During period 1, both the H^+ flux and the O^+ flux increased simultaneously. However, in period 2, the intensities were anti-correlated, with the O^+ intensity increasing when the H^+ intensity decreased. The anti-correlated energy-time dispersions are similar for O^+ and H^+ , suggesting that both O^+ and H^+ undergo similar drift motions. To examine these correlated and anti-correlated periods in more detail, we in-

vestigated the H^+ , O^+ and He^+ pitch-angle distributions. In panels 4–6 of Fig. 5, the pitch-angle distributions (0.04–0.2 keV) are displayed. From 14:55 UT–15:05 UT (period 1), we again observe bidirectional plasma outflows from the ionosphere from both hemispheres, similar to the event 1, but in this case, the outflow is more persistent and occurs for all three ion species. Mapped to the ionosphere, the outflow originates from an invariant latitude range in excess of 3° .

Panels 7–8, showing the net outflow of H^+ , O^+ and He^+ , confirm that there is an increase of the O^+ upgoing flux and a decrease of H^+ upgoing flux during period 2.

The number density plot (bottom panel in Fig. 5) shows higher densities for O^+ compared to the He^+ densities, indicating that the plasma originates from the lower part of the ionosphere.

Similar to event 1, the energy-time dispersed signatures and plasma outflows took place during low geomagnetic activities. The energy-time dispersed signatures were observed more than two days after a magnetic storm with a D_{st} peak at –221 nT (not shown here). AE was fairly small, as can be seen in panel 9. More than 48 h have passed since the last substorm activity of $\text{AE} > 500$ nT. IMF was weakly positive ($B_z \sim 0.3$ nT, Table 1). Minor high latitude auroral activity occurred around 6 h before our observation period (around 08:31 UT–08:50 UT). The high latitude activity occurred during northward IMF, suggesting minor influences on the ring current.

3.3 Event 3: 20 February 2002

Figure 6 shows data from 20 February 2002; the MLT varies between 0.6–0.7 during the study period. The pitch-angle distribution of H^+ , O^+ and He^+ are displayed in panels 3–5. The O^+ and He^+ distributions are bidirectional and rather similar, with fluxes peaking at $\leq 30^\circ$ and $\geq 150^\circ$, while H^+ displays a lack of bidirectional outflow from the hemispheres. The narrow O^+ and He^+ beams suggest ion outflow from low altitudes. On the other hand, the H^+ distribution is essentially isotropic. The isotropic H^+ distribution could in principle result from an isotropisation in the course of the H^+ outflow from a low-altitude source. On the other hand, it may also imply outflow from a low-altitude source with strong heavy ion dominance, especially O^+ , into a region of pre-existing isotropic H^+ ions. The latter seems more likely because the H^+ distribution also contains energy-time

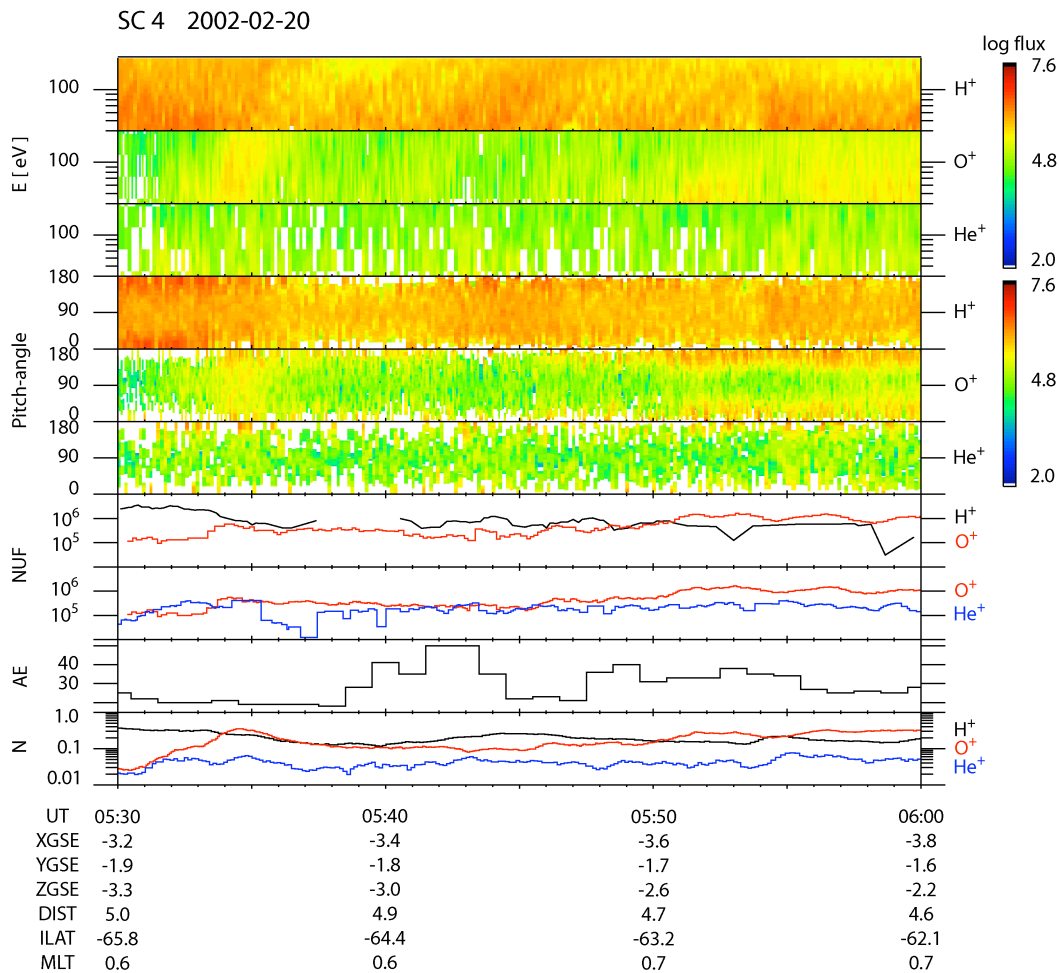


Fig. 6. Energy-time spectrograms, pitch-angle distributions $[(\text{cm}^2 \text{ s sr keV})^{-1}]$, net upgoing fluxes (NUF) in $[\text{cm}^{-2} \text{ s}^{-1}]$, AE in [nT] and density plot in $[\text{cm}^{-3}]$ in the low energy range of 40 eV to 200 eV for H^+ , O^+ and He^+ during the period from 05:30 UT through 06:00 UT, on 20 February 2002.

dispersed signatures. In the time period 05:34 UT–05:36 UT, there is a difference between the H^+ and the O^+ pitch-angle distributions; the O^+ flux increased while the H^+ flux decreased during the same time period. A similar difference between upgoing fluxes of H^+ and O^+ as that observed in the time period 2 (15:14 UT–15:20 UT) in Fig. 5 is observed in panel 7 of Fig. 6, i.e., an increase of the O^+ net upgoing flux when the H^+ net upgoing flux shows a decrease in the time period 05:34 UT–05:36 UT. The energy-time spectrograms of the three ion species in the top three panels show several other energy-time dispersed signatures for H^+ . Notice that all energy-time dispersed signatures are characterised by isotropic distributions, sometimes embedded in regions of field-aligned fluxes.

The number density plot in the bottom panel of Fig. 6 shows a higher abundance of O^+ than H^+ in the periods 05:34 UT–05:36 UT and 05:50 UT–06:00 UT. Our interpretation of the gradually increasing amount of O^+ is that of

a source region gradually moving towards lower altitudes, where O^+ becomes more abundant than H^+ . Nonetheless, the overall high abundance of O^+ compared to He^+ suggests a low altitude ionospheric origin.

The geomagnetic activities during this event are similar to events 1 and 2, i.e., occurring during geomagnetically quiet conditions. The event was observed approximately one day after a minor magnetic storm that had ceased during the time interval discussed. Furthermore, AE (panel 9 in Fig. 6) displayed small values during the event, and the nearest substorm activity was found 30 h before this event. Thus the AE indices before and during this event are even smaller than those for the 21 August 2001, and 26 November 2001, events. The IMF changed between weakly positive and weakly negative values ($B_z \sim \pm 1$ nT, Table 1). The timing of the energy-time dispersed signatures occurred almost at the same time as the IMF changed sign.

4 Summary and discussion

In the ring current, H^+ , O^+ and He^+ are the dominating ions. For obvious reasons, most studies have focused on the high-energy ring current ion component and its characteristics during geomagnetic disturbed conditions. In this paper, we have focused on sub-keV (40–200 eV) H^+ , O^+ and He^+ ions in the ring current. The origin and characteristics of these ions have been discussed. We observed three events during relatively quiet geomagnetic periods and different magnetic local time periods, 14.0–13.2 MLT at $L \sim 17.4$ –5.1, 7.1–6.9 MLT at $L \sim 6.5$ –4.5 and 0.6–0.7 MLT at $L \sim 5.9$ –4.6 (see Table 1), i.e., two events were observed on the dayside and one event on the nightside.

The three events in this paper occurred at three widely different magnetic local times and during relatively quiet geomagnetic periods. There were no major geomagnetic storms or substorms ten hours (or less) before the observations. At present, the common idea of how the energy-time dispersed signatures are created is based more or less on plasma injections from the nightside, caused by geomagnetic storms or substorms. After the nightside plasma injections, the ions then separate into two different drift directions. Depending on the energy, the ions will drift either westward or eastward (Yamauchi and Lundin, 2006). Intermediate energy ions experience a more complicated drift because of the competition between the westward gradient-curvature and the eastward $E \times B$ drifts. The eastward ion drift increases with decreasing ion energy. The gradient-curvature drift makes the eastward drift decrease for high energy ions. Therefore, higher energy ions are slower and appear later, causing the dispersive signature.

In this article, we argue that sub-keV ions may be supplied throughout the ion drift paths and mix with the local and freshly upgoing ions. Our observations show outflow from the ionosphere intermixed with drifting energy-time dispersed plasma signatures originating from a source earlier along the ion trajectory. In event 1, the features of the He^+ , panels 3 and 6 in Fig. 4, indicate such localised outflow into the ring current. We therefore argue that energy-time dispersed signatures may also be independent of the substorm activity but are formed as a consequence of the ion drifts.

The source region of the planetary ions may vary. For instance, the number density plot (bottom panel in Fig. 4) shows that the amount of He^+ is higher than the amount of O^+ . Since the ionosphere is stratified with respect to ion mass, this implies that the outflow in this case originates from a higher altitude, such as the plasmasphere or the polar wind. An argument for the plasmasphere as the more likely source is the transient feature of the combined H^+ and He^+ events, implying a more local insertion. Another, more circumstantial, alternative is that polar wind ions are transiently convected towards the dayside ring current ($B_z > 0$). On the other hand, panel 5 in Figs. 5 and 6 displays an outflow dominated by O^+ , implying a low-altitude ionospheric

origin below the crossover altitude where O^+ begins to dominate (e.g., Moore, 1980). Altogether, our observations indicate that the ionosphere and plasmasphere may provide a steady and potentially homogeneous (with respect to MLT) contribution of sub-keV ions into the ring current, occurring also during quiet times.

Ionospheric plasma accelerated upward is expected to maintain a field-aligned pitch-angle distribution further out in the magnetosphere. Such field-aligned, beamed, pitch-angle distributions were observed in all three events in this paper (see panel 6 in Fig. 4, panels 4–6 in Fig. 5 and panels 5–6 in Fig. 6). The observed field-aligned distributions therefore represent freshly upgoing terrestrial ions into the ring current. Narrow beams imply a magnetic connection to a low-altitude source region. Conversely, broad conical shaped ion distributions suggest a close proximity to the source (e.g., in the plasmasphere), but they may also imply beam-broadening by wave-induced transverse ion energising. With time, the ion beams are expected to gradually become isotropised as a result of wave-particle interaction, eventually taking the form of isotropic drifting sub-keV ion signatures. We therefore hypothesise that the energy-time dispersed signatures originate from upgoing ion distributions that have become isotropised. The isotropic component may subsequently evolve into energy-time dispersed signatures as a result of the combined gradient-curvature and $E \times B$ drift along the drift paths.

Eventually, the sub-keV ring current ions are subject to loss processes, such as charge exchange and ion precipitation back into the atmosphere. The fact that charge exchange processes are involved is evidenced by, e.g., Fig. 1, showing a strong decrease of sub-keV H^+ fluxes in the innermost part of the orbit. For low energies (< 1 keV), He^+ has a much smaller charge-exchange cross section than O^+ by a factor of 10 (Tinsley, 1981).

5 Conclusion

We have studied the outflow of ionospheric sub-keV ions, H^+ , He^+ and O^+ , as an additional source for the ring current population. Three events observed during different magnetic local times and with different characteristics have been investigated and discussed. Combining ion data from three Cluster spacecraft indicates that the energy-time dispersed signatures are foremost a spatial phenomenon. From our investigation, we conclude that: (1) sub-keV ions of terrestrial origin are supplied into the ring current also during quiet geomagnetic conditions; (2) the composition of the outflow implies an origin that covers an altitude interval from the low-altitude ionosphere to the plasmasphere, and (3) terrestrial ions are moving upward along magnetic field lines, at times forming narrow collimated beams, but frequently also as broad conical shaped distributions. With time, the ion beams/conics are expected to gradually become isotropised

as a result of wave-particle interaction, eventually taking the form of isotropic drifting sub-keV ion signatures. We therefore argue that the sub-keV energy-time dispersed signatures originate from field-aligned terrestrial ion energising and outflow that may occur at all local times and also persist during quiet times.

Acknowledgements. The Cluster project was carried out by ESA, and the Cluster II CIS instrument was supported by ESA and built by many institutions: CESR Toulouse as PI institute, IRF Kiruna, MPE Garching, IFSI Roma, MPAE (now MPS) Lindau, U Bern, U Washington, UNH, LPARL and UCB/SSL. The AE and D_{st} indices are provided by Data Analysis Center for Geomagnetism and Space Magnetism, Kyoto University. The ACE data are provided by NOAA ACE team. The work of TTG was supported by the Swedish National Space Board.

Topical Editor I. A. Daglis thanks J. Horwitz for his help in evaluating this paper.

References

- Balsiger, H., Eberhardt, P., Geiss, J., and Young, D. T.: Magnetic storm injection of 0.9- to 16-keV/e solar and terrestrial ions into the high-altitude magnetosphere, *J. Geophys. Res.*, 85(A4), 1645–1662, 1980.
- Chappell, C. R., Green, J. L., Johnson, J. F. E., and Waite Jr., J. H.: Pitch angle variations in magnetospheric thermal plasma – Initial observations from Dynamics Explorer-1, *Geophys. Res. Lett.*, 9(9), 933–936, 1982.
- Collin, H. L., Quinn, J. M., and Cladis, J. B.: An empirical static model of low energy ring current ions, *Geophys. Res. Lett.*, 20(2), 141–144, 1993.
- Ebihara, Y., Yamauchi, M., Nilsson, H., Lundin, R., and Ejiri, M.: Wedge-like dispersion of sub-keV ions in the dayside magnetosphere: Particle simulation and Viking observation, *J. Geophys. Res.*, 106(A12), 29571–29584, 2001.
- Ebihara, Y., Kistler, L. M., and Eliasson, L.: Imaging cold ions in the plasma sheet from the Equator-S satellite, *Geophys. Res. Lett.*, 35, L15103, doi:10.1029/2008GL034357, 2008.
- Fennell, J. F., Croley Jr., D. R., and Kaye, S. M.: Low-energy ion pitch angle distributions in the outer magnetosphere: Ion zipper distributions, *J. Geophys. Res.*, 86(A5), 3375–3382, 1981.
- Geiss, J., Balsiger, H., Eberhardt, P., Walker, H. P., Weber, L., and Young, D. T.: Dynamics of magnetospheric ion composition as observed by the GEOS mass spectrometer, *Space Sci. Rev.*, 22, 537–566, 1978.
- Horwitz, J. L.: Core plasma in the magnetosphere, *Rev. Geophys.*, 25(3), 579–587, 1987.
- Kaye, S. M., Shelley, E. G., Sharp, R. D., and Johnson, R. G.: Ion composition of zipper events, *J. Geophys. Res.*, 86(A5), 3383–3388, 1981.
- Lundin, R., Lyons, L. R., and Pissarenko, N.: Observations of the ring current composition at $L < 4$, *Geophys. Res. Lett.*, 7(6), 425–428, 1980.
- Maynard, N. C. and Chen, A. J.: Isolated cold plasma regions: Observations and their relation to possible production mechanisms, *J. Geophys. Res.*, 80, 1009–1013, 1975.
- Moore, T. E.: Modulation of terrestrial ion escape flux composition (by low-altitude acceleration and charge exchange chemistry), *J. Geophys. Res.*, 85(A5), 2011–2116, 1980.
- Moore, T. E., Lundin, R., Alcayde, D., Andre, M., Ganguli, S. B., Temerin, M., and Yau, A.: Source processes in the high-latitude ionosphere, Ch #2, in: *Magnetospheric Plasma Sources and Losses*, *Space Sci. Rev.*, 88, 7–84, 1999.
- Newell, P. T. and Meng, C.-I.: Substorm introduction of ≤ 1 -keV magnetospheric ions into the inner plasmasphere, *J. Geophys. Res.*, 91(A10), 11133–11145, 1986.
- Rème, H., Aoustin, C., Bosqued, J. M., et al.: First multispacecraft ion measurements in and near the Earth's magnetosphere with the identical Cluster ion spectrometry (CIS) experiment, *Ann. Geophys.*, 19, 1303–1354, 2001, <http://www.ann-geophys.net/19/1303/2001/>.
- Roelof, E. C., Mitchell, D. G., and Williams, D. J.: Energetic neutral atoms ($E \sim 50$ keV) from the ring current: IMP 7/8 and SSE 1, *J. Geophys. Res.*, 90(A11), 10991–11008, 1985.
- Sauvaud, J. A., Crasnier, J., Mouala, K., Kovrazhkin, R. A., and Jorjio, N. V.: Morning sector ion precipitation following substorm injections, *J. Geophys. Res.*, 86(A5), 3430–3438, 1981.
- Shelley, E. G., Johnson, R. G., and Sharp, R. D.: Satellite observations of energetic heavy ions during a geomagnetic storm, *J. Geophys. Res.*, 77(31), 6104–6110, 1972.
- Stern, D. P.: The motion of a proton in the equatorial magnetosphere, *J. Geophys. Res.*, 80, 595–599, 1975.
- Tinsley, B. A.: Neutral atom precipitation – a review, *J. Atmos. Terr. Phys.*, 43(5/6), 617–632, 1981.
- Vallat, C., Ganushkina, N., Dandouras, I., Escoubet, C. P., Taylor, M. G. G. T., Laakso, H., Masson, A., Sauvaud, J.-A., Rème, H., and Daly, P.: Ion multi-nose structures observed by Cluster in the inner Magnetosphere, *Ann. Geophys.*, 25, 171–190, 2007, <http://www.ann-geophys.net/25/171/2007/>.
- Volland, H.: A semiempirical model of large-scale magnetospheric electric fields, *J. Geophys. Res.*, 78, 171–180, 1973.
- Williams, D. J.: The Earth's ring current: causes, generation, and decay, *Space Sci. Rev.*, 34, 223–234, 1983.
- Yamauchi, M., Lundin, R., Eliasson, L., and Norberg, O.: Meso-scale structures of radiation belt/ring current detected by low-energy ions, *Adv. Space Res.*, 17(2), 171–174, 1996.
- Yamauchi, M., Lundin, R., Eliasson, L., Winningham, D., Reme, H., Vallat, C., Dandouras, I., et al.: Structures of sub-keV ions inside the ring current region, *The Inner Magnetosphere: Physics and Modeling*, *Geophysical Monograph Series 155*, 41–46, 2005.
- Yamauchi, M. and Lundin, R.: Sub-keV ring current ions as the tracer of substorm injection, *Ann. Geophys.*, 24, 355–366, 2006, <http://www.ann-geophys.net/24/355/2006/>.
- Yamauchi, M., Brandt, P. C., Ebihara, Y., Dandouras, I., Nilsson, H., Lundin, R., Rème, H., Vallat, C., Lindqvist, P.-A., Balogh, A., and Daly, P. W.: Source location of the wedge-like dispersed ring current in the morning sector during a substorm, *J. Geophys. Res.*, 111, A11S09, doi:10.1029/2006JA011621, 2006.